Absolute phase-assisted three-dimensional data registration for a dual-camera structured light system

Song Zhang and Shing-Tung Yau

Mathematics Department, Harvard University, One Oxford Street, Cambridge, Massachusetts 02138, USA

*Corresponding author: szhang77@gmail.com

Received 3 January 2008; revised 10 April 2008; accepted 2 May 2008;
posted 8 May 2008 (Doc. ID 91223); published 2 June 2008

For a three-dimensional shape measurement system with a single projector and multiple cameras, registering patches from different cameras is crucial. Registration usually involves a complicated and time-consuming procedure. We propose a new method that can robustly match different patches via absolute phase without significantly increasing its cost. For y and z coordinates, the transformations from one camera to the other are approximated as third-order polynomial functions of the absolute phase. The x coordinates involve only translations and scalings. These functions are calibrated and only need to be determined once. Experiments demonstrated that the alignment error is within RMS 0.7 mm. © 2008 Optical Society of America

OCIS codes: 110.6880, 120.2650, 120.3940, 120.5800.

1. Introduction

High-resolution, large-range 3D shape measurement is crucial for various applications, including manufacturing, medical imaging, entertainment, computer graphics, and computer vision.

A structured light system is different from a stereo system in that one of the cameras of the stereo system is replaced with a projector to illuminate structured patterns used to solve the fundamental stereo-matching problem [1]. For a structured light system using a method based on phase shifting, the projected sinusoidal fringe patterns become an analog signal once the projector is defocused. The spatial resolution is dependent only on the sampling of the camera; i.e., it is determined by the camera resolution. Therefore, to increase the spatial measurement resolution, the camera resolution has to be increased. However, for a single-camera system, increasing the spatial measurement resolution usually compromises the scanning range. Moreover, the camera resolution has its limits. In contrast, a multiple-camera system can increase the measurement range as well as its spatial resolution by using each camera to measure a partial area of the object.

For a single-camera structured light system, the 3D coordinates can be obtained once the system is calibrated [2,3]. In principle, a structured light system with multiple cameras can generate the data points in the same world coordinate system if the system is calibrated precisely. However, in practice, because of the calibration error and/or measurement error, the measurement results from different cameras may have some difference, which is the case for our system. Therefore, 3D registration (or matching) is necessary to guarantee that the output measurement data points are in the same world coordinate system for complete a 3D view [4–7].

Various researchers have proposed different registration approaches, including using an iterative closest point algorithm [8,9], a photogrammetric technique [10], a self-calibration method [11], and moving objects in multiple overlapping measurement positions together with a special 3D calibration [12,13]. However, reliable, rapid, general purpose 3D registration is still a difficult and open problem.

0003-6935/08/173134-09$15.00/0

For a system using a single projector, the registration problem is simplified, since the structured patterns provide constraints for it. For a phase-shifting-based method, the absolute phase can be used to assist the registration. In the absolute phase domain, the phase obtained from the camera images and that from the computer generated projection fringe images are the same. Therefore, if the phase is absolute, the absolute phase line captured by any camera viewing from any angle at the same moment (i.e., the object relative to the imaging system does not change during image acquisition) should remain the same.

Absolute phase has been extensively utilized for diverse purposes, such as absolute 3D coordinate measurement [14], structured light system calibration [2,3], and structured light system self-calibration [11,15]. Yalla and Hassebrook introduced techniques for using overlapping X_p and Y_p phase values to align the surfaces scanned by two projectors and viewed by a single camera [16]. Wang *et al.* proposed a system using multiple cameras for accurate depth measurement [17]. In this technique, the absolute phase is used to assist the corresponding point detections based on epipolar geometry. Wang *et al.* demonstrated that it is a very good technique for accurate 3D shape measurement. However, since both cameras must see the point to be measured, the measurement range is actually less than for a single-camera system. Therefore, this technique improves the measurement accuracy by sacrificing the measurement range. Moreover, because a multifrequency phase-shifting algorithm is used, it is very difficult for them to reach real-time 3D shape measurement. In the work of Schreiber and Notni [15], where more than two cameras are used, rotation of the projector is required for one scan with a self-calibrating functionality realized. For static object measurement, their system can achieve very high accuracy and flexibility. However, this technique requires many (many more than three) fringe images and involves projector rotation to complete the measurement. Therefore, it is very difficult to perform the measurement at high speed.

Our research focuses on developing a real-time 3D shape measurement system. We have successfully developed a single-camera system that can perform the measurement at speeds up to 60 frames/s [14,18] using a fast three-step phase-shifting algorithm [19]. However, a single-camera system can measure the 3D geometry only from a single view. To extend its measurement range, a dual-camera system has been developed [20]. In this system, two cameras acquire fringe images simultaneously at a high speed (180 frames/s), and each camera generates one piece of the 3D geometry separately and independently. Since a three-step phase-shifting algorithm is used, three fringe images can be used to reconstruct one 3D geometry. Therefore, the measurement speed is 60 frames/s. The advantages of this system are that (1) two cameras simultaneously perform the measurement independently, and therefore the measurement speed is not reduced in comparison with a single-camera system, and (2) the measurement range is increased because each camera captures its viewing areas. However, this system uses an iterative closest point algorithm to register two pieces of 3D geometries. The iterative closest point technique performs well for single-frame registration. We found that it is difficult for this algorithm to obtain consistent results from frame to frame. Therefore, a systematic consistent approach has to be developed for our real-time 3D video scanning system.

In this research, we show that the absolute phase is a very powerful tool for such a matching problem. The relationships between the measured 3D points of the left-hand camera and those of the right-hand camera can be established by calibration. We found that these relationships can be described as third-order polynomial functions of absolute phase for y and z coordinates independently. For x coordinates, only translation and scaling of the original data is required. These functions can be obtained by calibration and only need to be determined once. Therefore, consistent registration from frame to frame can be ensured. Experiments are presented to demonstrate the performance of the proposed method. For our structured light system with dual cameras, the alignment error is within RMS 0.7 mm.

Section 2 introduces the basics of the 3D matching algorithm. Section 3 describes the 3D shape measurement system used to verify the proposed algorithm. Section 4 introduces the phase-shifting algorithm used for this research. Section 5 explains the system calibration approach used. Section 6 addresses the matching algorithm used in this research. Section 7 presents experimental results, and Section 8 summarizes this work.

2. Principle

Before introducing our technology, we clarify some terminology that will be used in the remaining text.

- *Projection phase* ϕ^p: phase obtained from the fringe image generated by the computer and before its projection.
- *Camera phase* ϕ: phase obtained from the fringe images captured by the camera using the phase-wrapping and -unwrapping algorithms. This phase is called relative phase and is also regarded as the phase in a phase-shifting algorithm.
- *Absolute phase* ϕ_a: one or more points have known phase value; the relative phase obtained from phase-shifting algorithms is converted to absolute phase so that these specified points have the predefined phase values.

In this research, the absolute phase ϕ_a is determined by encoding a marker point in the projected fringe images with an absolute phase value of 0. Once the marker point is detected, the absolute phase between the captured image and the projected image is uniquely correlated; i.e., in the absolute phase

domain, the phase obtained from the camera images and that from the computer-generated fringe images are the same. Therefore, if the phase is absolute, the absolute phase line captured by any camera viewing from any angle at the same moment (i.e., the object relative to the imaging system does not change during image acquisition) should remain the same. We found that this is very powerful tool for 3D data matching for our system.

Figure 1 shows a typical example of one projection line. The projection line, the dashed lines in the figure, is imaged from two different cameras and has different deformations. Although the images captured from different cameras are different, the curve is unique on the object. Therefore, the matching is optimal if these two curves are matched, because they are physically the same. However, from one directional absolute phase in itself, the matching is not unique, since any point on the curve has the same absolute phase. In this research, the marker point, used for the relative phase to absolute phase conversion, is also used as the constraint for the alignment in one direction.

3. System Description

Figure 2 shows the setup of the structured light system with a single projector and dual cameras. The projector projects computer-generated phase-shifted fringe images onto the object; two cameras viewing from different angles image the deformed fringe images that are further processed by software through phase-wrapping and -unwrapping algorithms. 3D coordinates can be obtained from the phase once the system is calibrated. Each camera captures one 3D patch within its view under its own coordinate system. Two patches have to be matched and merged into a single piece of 3D data meshes (or point clouds) for further data analysis.

In this research, we developed a structured light system with dual cameras. The projector we used is a digital light processing projector (PLUS U5-632h) with a resolution of 1024×748, the cameras

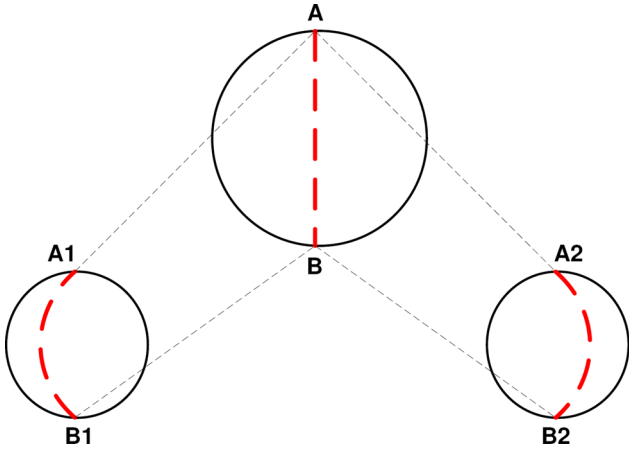

Fig. 1. (Color online) One projection line will be imaged to yield different lines for different cameras viewed from different viewing angles.

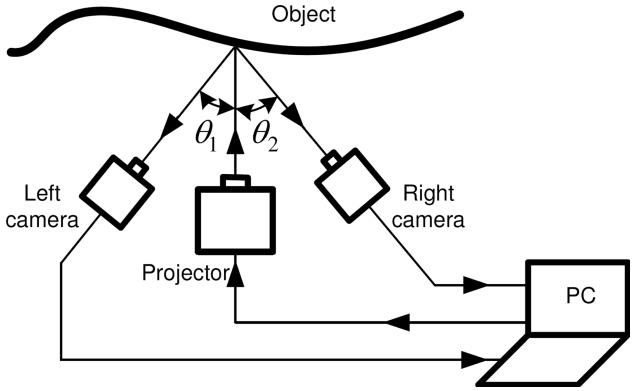

Fig. 2. System setup for structured light with one projector and dual cameras.

are digital CCD cameras with an image resolution of 640×480 (Pulinx TM6740-CL), and the frame grabber is Matrox Solios XCL with camera link interface. Figure 3 shows the photograph of our system.

4. Three-Step Phase-Shifting Algorithm

Over the years, various phase-shifting algorithms, including three-step, four-step, and double-three-step algorithms, have been developed [21]. Phase-shifting-based algorithms are extensively employed for optical metrology because of their speed and non-surface-contact nature. In general, the more fringe images are used, the better the measurement that can be achieved. However, using more fringe images will reduce the data acquisition speed. For real-time 3D shape measurement, a three-step phase-shifting algorithm is usually used [18].

Since our research focuses on developing a real-time 3D shape measurement system, the measurement speed plays a key role. In this research, we use a three-step phase-shifting algorithm with a phase shift of $2\pi/3$ for its speed and simplicity:

$$I_1 = I'(x,y) + I''(x,y)\cos[\phi(x,y) - 2\pi/3], \quad (1)$$

$$I_2 = I'(x,y) + I''(x,y)\cos[\phi(x,y)], \quad (2)$$

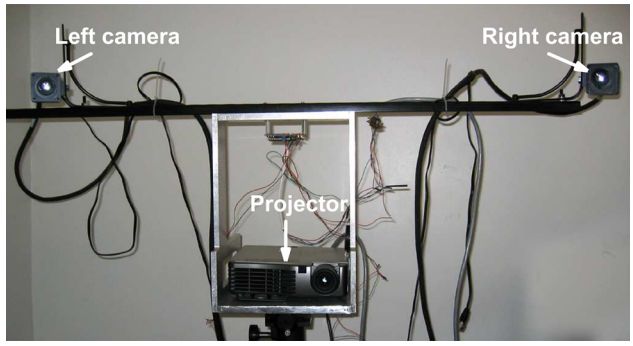

Fig. 3. (Color online) Photograph of the real measurement system.

$$I_3 = I'(x,y) + I''(x,y)\cos[\phi(x,y) + 2\pi/3], \quad (3)$$

where $I'(x,y)$ is the average intensity, $I''(x,y)$ the intensity modulation, and $\phi(x,y)$ the phase to be solved for. Phase $\phi(x,y)$ can be computed from Eqs. (1)–(3),

$$\phi(x,y) = \tan^{-1}\left[\frac{\sqrt{3}(I_1 - I_3)}{2I_2 - I_1 - I_3}\right]. \quad (4)$$

3D information is carried in the phase, $\phi(x,y)$, whose value ranges from $-\pi$ to $+\pi$. This step is also called phase wrapping. If multiple fringe stripes are used, a phase unwrapping algorithm has to be adopted to obtain the continuous phase map [22]. In this research, our previously developed phase unwrapping algorithm is implemented in our system [23].

However, in general, the phase unwrapping from a single wrapped phase map can obtain the only relative phase, i.e., relative to one point on the map. To uniquely know the phase value (also called absolute phase ϕ_a), at least one point on one connected component has to be known. We encoded a marker into the projected fringe images, which corresponds to absolute phase 0 [14]. For any measurement, after phase unwrapping, assuming that the marker point has phase ϕ_0, the whole phase map is shifted ($\phi_a = \phi - \phi_0$) to guarantee that the marker point has absolute phase 0. Once the absolute phase is known, the absolute coordinates can be obtained once the system is calibrated [2,3].

5. System Calibration

In this research, we calibrate the system by using the extension of the calibration method introduced in [2]. The intrinsic parameters of the projector and the cameras are calibrated by using a standard red and blue flat checkerboard. The extrinsic parameters are estimated from the same physical position of the calibration board to ensure they are in the same world coordinate system. Only a linear pinhole camera model is used in this research for all calibration. After calibration, we obtain three 3×4 matrices, M^l, M^r, and M^p, which transform the world coordinates into the image coordinates according to the following equations:

$$s^{cl}[u^{cl}, v^{cl}, 1]^T = M^l[x^w, y^w, z^w, 1]^T, \quad (5)$$

$$s^{cr}[u^{cr}, v^{cr}, 1]^T = M^r[x^w, y^w, z^w, 1]^T, \quad (6)$$

$$s^{cp}[u^{cp}, v^{cp}, 1]^T = M^p[x^w, y^w, z^w, 1]^T, \quad (7)$$

where s^c is a constant, $[u, v, 1]^T$ the homogeneous image coordinates, and $[x^w, y^w, z^w, 1]$ the homogeneous world coordinates. Superscripts l, r, and p indicate the left-hand camera, right-hand camera, and projector, respectively. For each projector–camera pair, we can obtain the absolute coordinates point by point from the absolute phase [2]. Theoretically, if the whole system is calibrated in the same world coordinate system, then each projector–camera pair should generate the same world coordinate for the same point, and the alignment should be automatic. However, owing to the calibration error and/or measurement error, the measured results are not in the same world coordinate system. Therefore, 3D data matching for the two projector–camera pairs is necessary.

6. Three-Dimensional Data Matching

Figure 4 illustrates the process of the matching algorithm used in our research. From the absolute phases of the left-hand camera (ϕ_a^l) and right-hand camera (ϕ_a^r), the absolute coordinates can be computed as $C^l(x,y,z)$ and $C^r(x,y,z)$, respectively. Meanwhile, these absolute phase maps can be converted to projector absolute phase (ϕ_a^p) in the projection image domain, where the absolute phase is also ϕ_a. From the absolute phase, ϕ_a, coordinates from the left-hand camera, $C^l(x,y,z)$, and the right-camera, $C^r(x,y,z)$, are correlated and converted to the same world system $C(x,y,z)$. Once these relationships are established, they can be applied for the future measurement.

The matching procedure is to establish the relationship between coordinates of the left-hand camera and their corresponding coordinates of the right-hand camera. In this research, we treat x, y, and z coordinates independently for matching and choose the coordinate system in the left-hand camera as the world coordinate system for both cameras, i.e., $C(x,y,z) = C^l(x,y,z)$. Therefore, three functions,

$$\delta x(\phi_a) = x^l - x^r = f_x(\phi_a), \quad (8)$$

$$\delta y(\phi_a) = y^l - y^r = f_y(\phi_a), \quad (9)$$

$$\delta z(\phi_a) = y^l - y^r = f_z(\phi_a), \quad (10)$$

are to be found. These functions are estimated by measuring a calibration flat board. The same flat checkerboard used for system calibration is measured by both cameras. The absolute phases and coordinates for each point are computed. Assuming one absolute phase line with an absolute phase value of ϕ_k, all measurement points with this absolute phase value from the left-hand camera and the right-hand camera are $(x_i^l, y_i^l, z_i^l)|_{\phi_k}$ $(i = 1 \ldots N)$ and $C^r(x,y,z)|_{\phi_k}$ $(j = 1 \ldots M)$, respectively, then

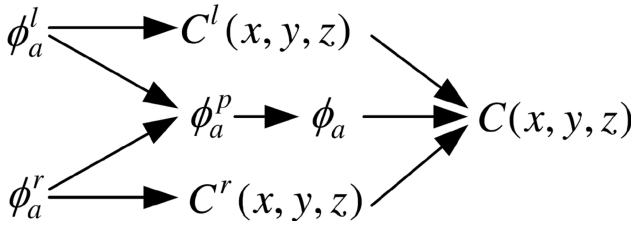

Fig. 4. Matching process.

$$\delta x(\phi_k) = \sum_{i=1}^{N} x_i^r/N - \sum_{j=1}^{M} x_j^l/M, \quad (11)$$

$$\delta y(\phi_k) = \sum_{i=1}^{N} y_i^r/N - \sum_{j=1}^{M} y_j^l/M, \quad (12)$$

$$\delta z(\phi_k) = \sum_{i=1}^{N} z_i^r/N - \sum_{j=1}^{M} z_j^l/M. \quad (13)$$

The coordinates of the right-hand camera can then be converted into the world coordinates by using the following equations:

$$x = x^r + f_x(\phi_a), \quad (14)$$

$$y = y^r + f_y(\phi_a), \quad (15)$$

$$z = z^r + f_z(\phi_a). \quad (16)$$

These functions have to be calibrated before any measurement. To simplify this problem, instead of using a uniform flat board, we use the same red and blue checkerboard as the standard calibration target. The advantage of using the red and blue checkerboard is not only that the coordinates for each point are known, but that the actual distance between each checker corner is also known. Our camera is black and white; thus the red and blue checker squares are barely seen from the camera's point of view. Therefore, the measurement is not significantly affected by them. Figure 5 shows checkerboard images of two cameras with a checker square size of 15 mm × 15 mm. In Fig. 5, horizontal lines represents one absolute phase value ($\phi_a = 30\pi$ rad) on the left- and the right-hand camera images. A set of absolute phase lines can be found, as well as their corresponding coordinates for each set of camera data.

Figure 6 shows the relationship between the absolute phase and the coordinates difference. We found that fitting the functions by using third-order polynomials is sufficient to fit $f_y(\phi_a)$ and $f_z(\phi_a)$ for our system. That is,

$$\delta_y \phi_a = f_y(\phi_a) = c_{y0} + c_{y1}\phi_a + c_{y2}\phi_a^2 + c_{y3}\phi_a^3, \quad (17)$$

$$\delta_z \phi_a = f_z(\phi_a) = c_{z0} + c_{z1}\phi_a + c_{z2}\phi_a^2 + c_{z3}\phi_a^3. \quad (18)$$

Here c_{yk}, c_{z_k}, $k = 0, 1, 2, 3$, are constants.

Figure 7 is the plot of δ_x with respect to ϕ_a. It can be seen that δ_x is almost independent of ϕ_a. This is because the fringe line is along the x axis and the phase does not change along the x direction. We found that, along the x direction, this function is a linear function with respect to x, which can be easily calibrated by measuring a set of fixed points with known dimensions along the x axis. Once these functions in Eqs. (8)–(10) are known, the coordinates for the left-hand camera can be transferred to the right-hand camera by using Eqs. (14)–(16).

Figure 8 shows the absolute phase lines from the left- and the right-hand camera with x and y values as the computed coordinates, where the dashed lines are from the left-hand camera and the solid lines are from the right camera. It can be seen here that before matching, the absolute phase lines are not aligned as expected (as shown in Fig. 8(a)). Figure 8(b) shows the result after alignment. Figure 8(b) clearly shows that the two absolute phase maps are aligned well after matching.

7. Experiments

To verify the performance of the proposed method, we first measured the checkerboard as shown in Fig. 5. We picked the 134 corners manually from the 2D images of the left- and right-hand cameras, as shown in Fig. 9, whose coordinates are obtained

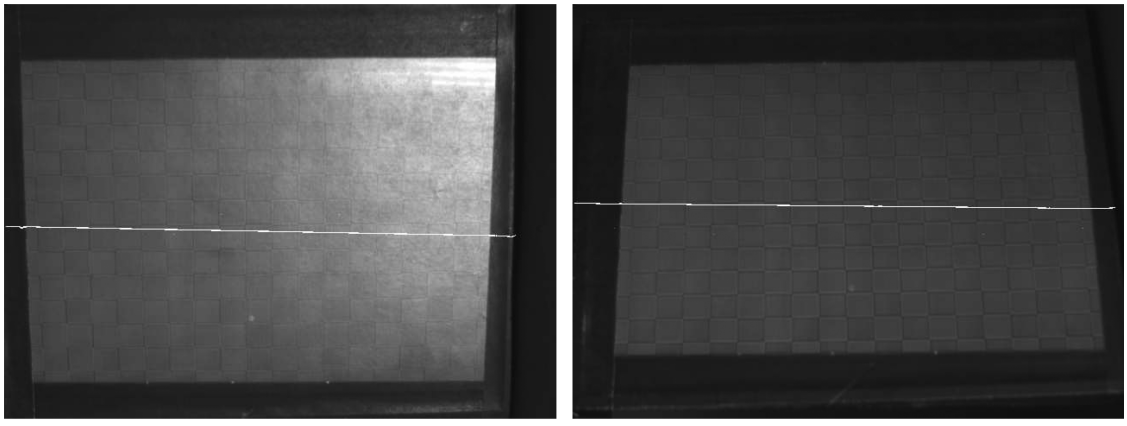

(a) (b)

Fig. 5. Calibration images of two cameras. The white line is an absolute phase line with absolute phase value of 30π rad. (a) Left camera image. (b) Right camera image.

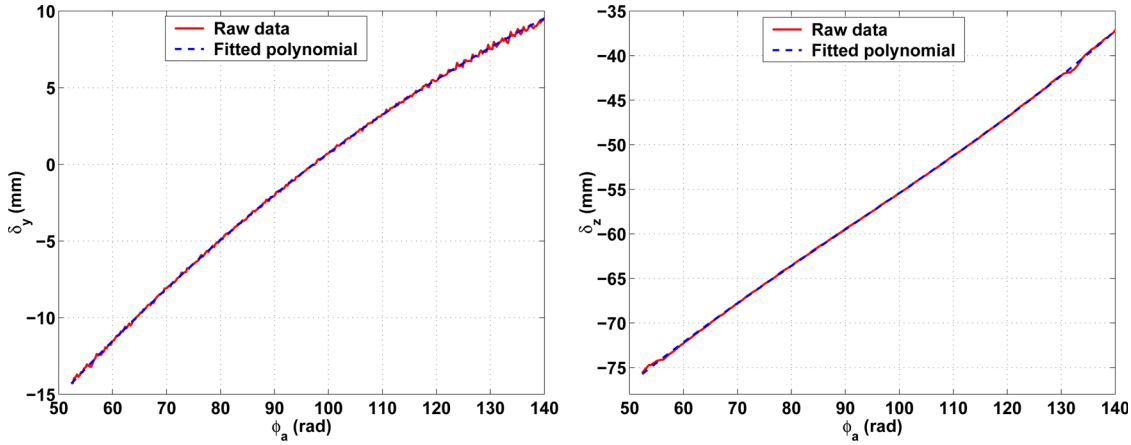

Fig. 6. (Color online) Polynomial fittings of δ_y and δ_z with respect to ϕ_a: (a) $\delta_y(\phi_a)$, (b) $\delta_z(\phi_a)$.

after coordinate computations. The corner x, y coordinates before matching are plotted in Fig. 9(a). It can be clearly seen that they are far from each other; the error is significant. The result after matching is shown in Fig. 9(b); the corner points are closely overlapping with each other for the corresponding pairs.

These checker corners (Fig. 10) are plotted on a 2D plane in Fig. 11 . After matching, the RMS error for all 134 of these corner points is 0.7 mm, which is already very good, since the measurement error for a single camera is approximately RMS 0.3 mm. It should be noted that in this experiment we used linear models for both the camera and the projector. The error is smaller in the center of the image, while it is larger for the outer areas [24]. This is consistent with our alignment; the largest error points occur on the outer points of the image.

Using the calibrated functions from the checkerboard data, we tested a more complicated model, as shown in Fig. 12. Figures 12(a) and 12(b) show 3D geometries from the left- and the right-hand camera, respectively. Figure 12(c) shows the two geometries rendered in the same scene. Where the darker (gray) color shows the 3D geometry from the left-hand camera, the brighter (peach) color shows the geometry from the right-hand camera. It can be seen that they are not aligned well. After matching, the two geometries are again rendered together in Fig. 12(d), where the two geometries overlap each other and the alignment is very good. Figure 12(e) shows another viewing angle after matching, and Fig. 12(f) shows two geometries rendered in wireframe mode after matching. This experiments demonstrated that the calibration functions [Eqs. (8)–(10)] only need to be calibrated once and applied to the remaining measurement, as long as the system configuration is not changed.

We should mention that this matching algorithm requires at least one preknown corresponding point on the left-hand camera and the right-hand camera, which is used to align the fringe line direction (x direction in our case). For our measurement system, we used a small marker as the corresponding point. The same point, the white markers inside the ellipse shown Fig. 13, is also used to convert the phase to absolute phase. These experiments demonstrate that our proposed method can match two 3D patches from two cameras satisfactorily.

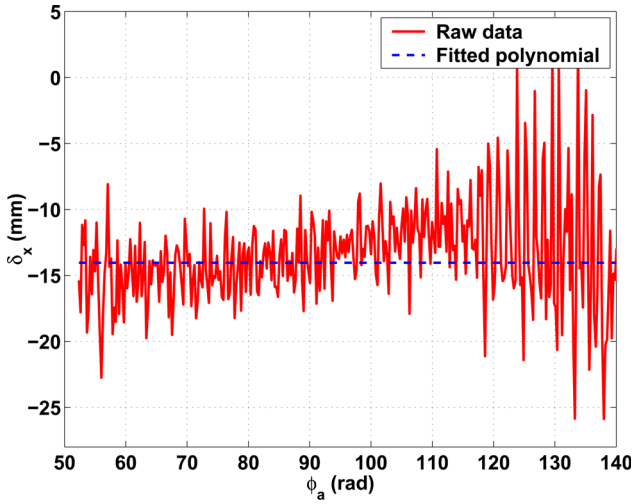

Fig. 7. (Color online) Polynomial fittings of δ_x with respect to ϕ_a.

8. Conclusions

This paper has presented a 3D data registration algorithm for a three-dimensional shape measurement system with a single projector and dual cameras. We introduced a new method that was able to robustly match different patches via absolute phase. In the absolute phase domain, the phase obtained from the camera-captured images and that from the computer-generated projection fringe images are the same. If the phase is absolute, the absolute phase line for capture by any camera viewing from any angle at the same moment should remain the same. Therefore, the matching can be performed by matching the absolute phase lines. In this research, we used polyno-

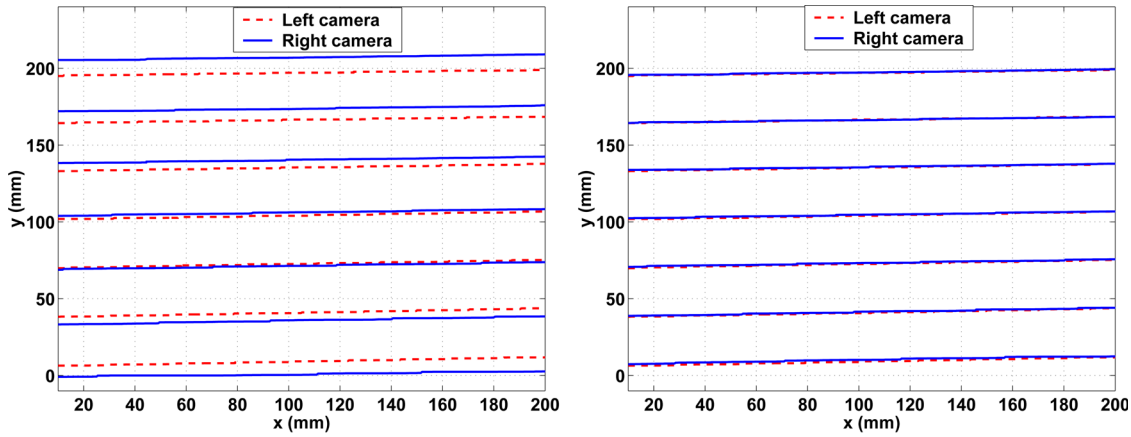

Fig. 8. (Color online) Absolute phase lines, from bottom to top, with an absolute phase value of $\phi_2 = 0\pi, 24\pi, ..., 44\pi$. (a) Before alignment. (b) After alignment.

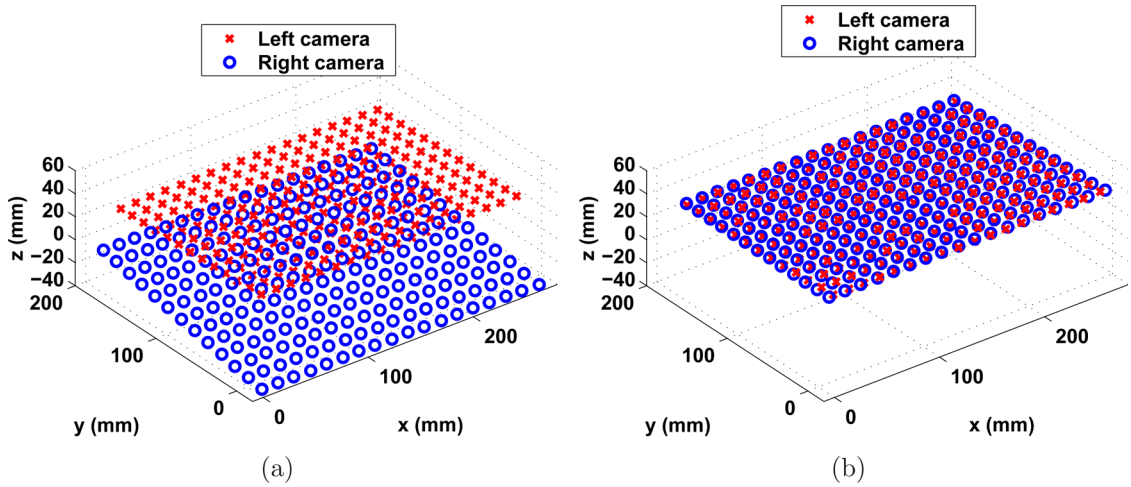

Fig. 9. (Color online) Corner coordinates of the checkerboard. (a) Before matching. (b) After matching.

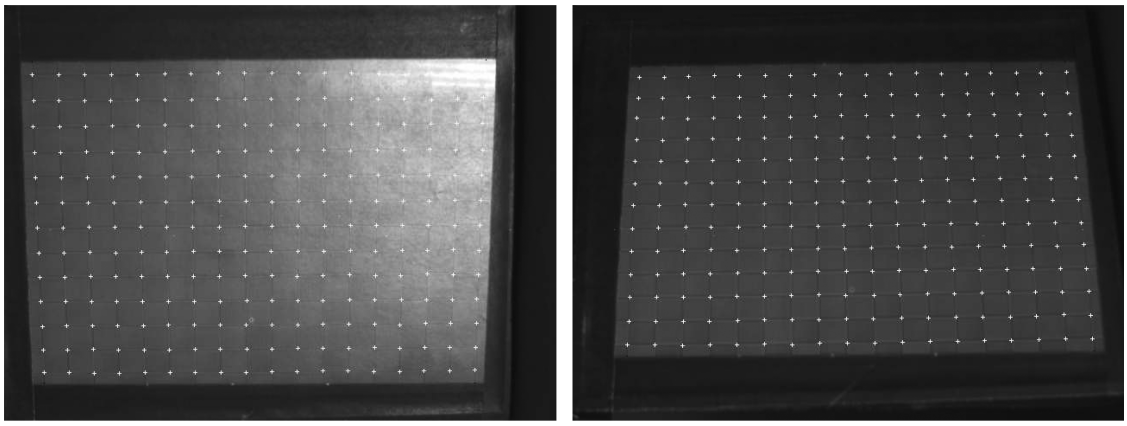

Fig. 10. Corners of the checkerboard.

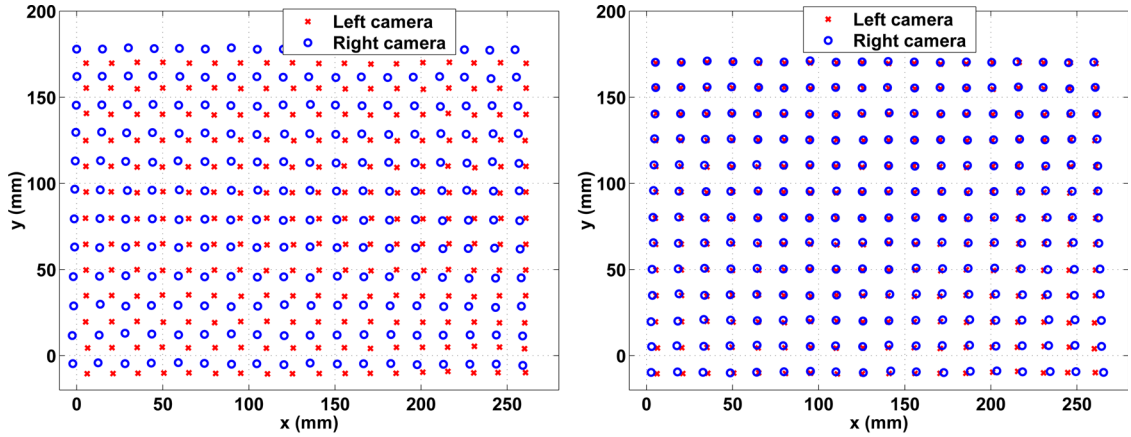

Fig. 11. (Color online) Corner coordinates of the checkerboard in a 2D plane. (a) Before matching. (b) After matching (RMS 0.7 mm).

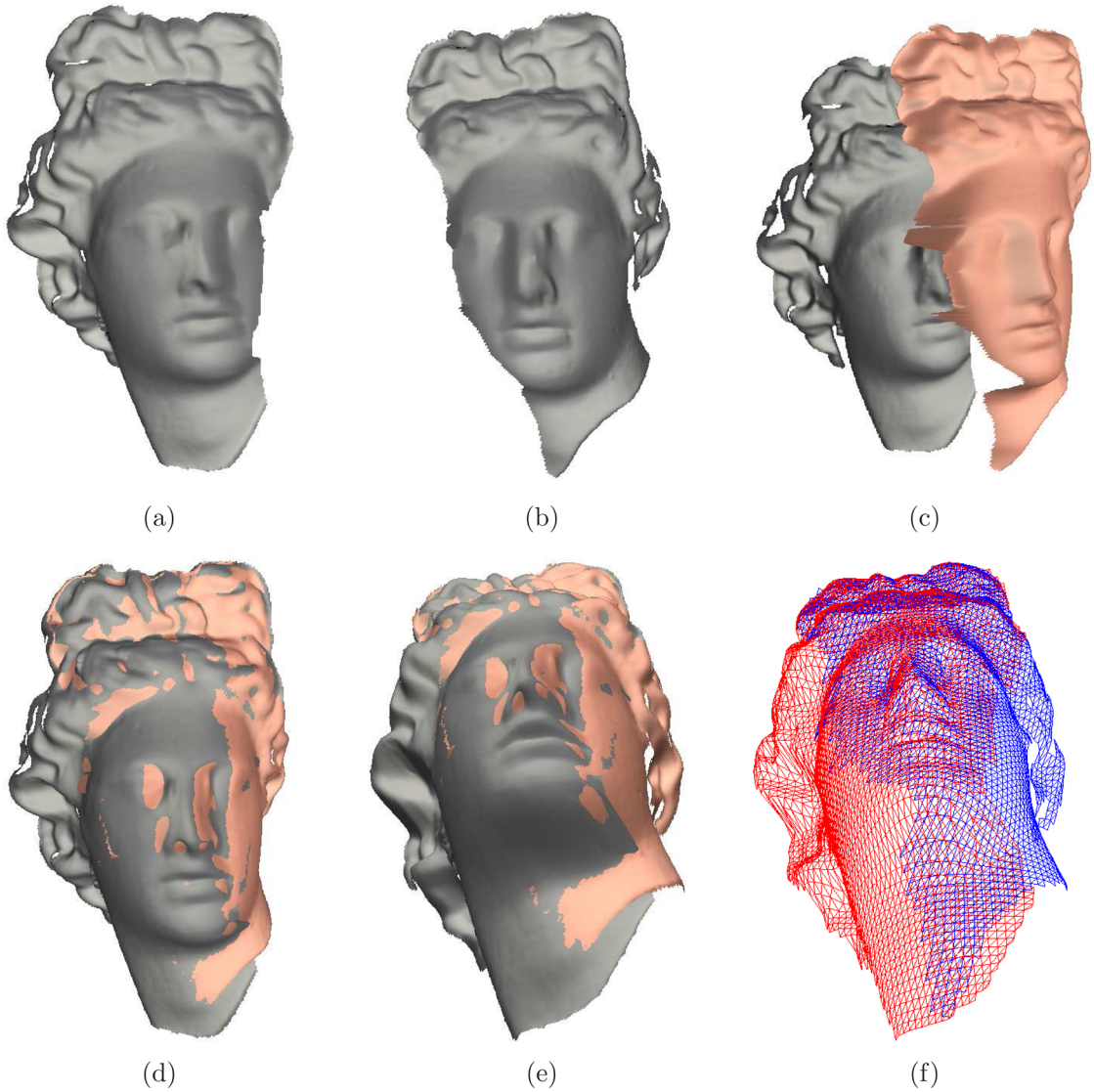

Fig. 12. (Color online) Measurement result for a more complicated object. (a) 3D geometry from the left-hand camera. (b) 3-D geometry obtained from the right-hand camera. (c) Before matching, two geometries rendered in the same scene. (d) After matching, two geometries rendered together. (e) After matching, two geometries rendered from another viewing angle. (f) After matching, two geometries rendered in wireframe mode.

(a) (b)

Fig. 13. (Color online) 2D photos of head sculpture from two cameras. (a) 2D photo from left-hand camera. (b) 2D photo from right-hand camera.

mial functions of absolute phase to represent the transformation for each measurement point for y and z coordinates. For x coordinates, the simple translation and scaling of x-axis coordinates was sufficient. These functions were calibrated by measuring a flat red and blue checkerboard. For our system, experiments demonstrated that the proposed method can successfully match the measurement results from different cameras for an arbitrary object with high accuracy (approximately RMS 0.7 mm when the single-camera–projector system measurement error is 0.3 mm).

References

1. J. Salvi, J. Pagès , and J. Batlle, "Pattern codification strategies in structured light systems," Pattern Recogn. **37**, 827–849 (2004).
2. S. Zhang and P. S. Huang, "Novel method for structured light system calibration," Opt. Eng. **45**, 083601 (2006)
3. R. Legarda-Sáenz, T. Bothe, and W. P. Jüptner, "Accurate procedure for the calibration of a structured light system," Opt. Eng. **43**, 464–471 (2004).
4. C. Reich, "Photogrammetrical matching of point clouds for 3D measurement of complex objects," Proc. SPIE **3520**, 100–110 (1998).
5. R. Massen, J. Gässler, C. Konz, and H. Richter, "From a million of dull point coordinates to an intelligent CAD description," *Proceedings of the Second International Workshop on Automatic Processing of Fringe Patterns*, W. Jüptner and W. Osten, eds. (Wiley, 1993), pp. 194–203.
6. H. Schöfeld, G. Häusler, and S. Karbacher, "Reverse engineering using optical 3D sensors," Proc. SPIE **3313**, 115–125 (1998).
7. P. J. Neugebauer, "Reconstruction of real-world objects via simultaneous registration and robust combination of multiple range images," Int. J. Shape Model. **3**, 71–90 (1997).
8. P. J. Besl and H. D. McKay, "A method for registration of 3-D shapes," IEEE Trans. Pattern Anal. Mach. Intell. **14**, 239–256 (1992).
9. Y. Chen and G. Medioni, "Object modelling by registration of multiple range images," Image Vision Comput. **10**, 145–155 (1992).
10. H. A. Beyer, V. Uffenkamp, and G. van der Vlugt, "Quality control in industry with digital photogrammetry," in *Optical 3D-Measurement Techniques III* (Wichmann, 1995), pp. 29–38.
11. V. Kirschner, W. Schreiber, R. Kowarschik, and G. Notni, "Self-calibrating shape measuring system based on fringe projection," Proc. SPIE **3102**, 5–13 (1997).
12. H. Kühmstedt, G. Notni, W. Schreiber, and J. Gerber, "Full-hemisphere automatic optical 3D measurement system," Proc. SPIE **3100**, 261–265 (1997).
13. A. K. Asundi and W. Zhou, "Mapping algorithm for 360-deg profilometry with time delayed integration imaging," Opt. Eng. **38**, 339–344 (1999).
14. S. Zhang and S.-T. Yau, "High-resolution, real-time 3D absolute coordinate measurement based on a phase-shifting method," Opt. Express **14**, 2644–2649 (2006).
15. W. Schreiber and G. Notni, "Theory and arrangements of self-calibrating whole-body three-dimensional measurement systems using fringe projection technique," Opt. Eng. **39**, 159–169 (2000).
16. V. Yalla and L. G. Hassebrook, "A novel geometric calibration technique for scalable multi-projector displays," Technical Report CSP-06-010 (University of Kentucky, 2006).
17. Y. Wang, K. Liu, Q. Hao, D. Lau, and L. G. Hassebrook, "Multi-camera phase measuring profilometry for accurate depth measurement," Proc. SPIE **6555**, 655509 (2007).
18. S. Zhang and P. S. Huang, "High-resolution, real-time three-dimensional shape measurement," Opt. Eng. **45**, 123601 (2006).
19. P. S. Huang and S. Zhang, "Fast three-step phase shifting algorithm," Appl. Opt. **45**, 5086–5091 (2006).
20. S. Zhang and S.-T. Yau, "Three-dimensional shape measurement using a structured light system with dual cameras," Opt. Eng. **47**, (1), 013604 (2008).
21. D. Malacara, ed., *Optical Shop Testing* (Wiley, 1992).
22. D. C. Ghiglia and M. D. Pritt, *Two-Dimensional Phase Unwrapping: Theory, Algorithms, and Software* (Wiley, 1998).
23. S. Zhang, X. Li, and S.-T. Yau, "Multilevel quality-guided phase unwrapping algorithm for real-time three-dimensional shape reconstruction," Appl. Opt. **46**, 50–57 (2007).
24. P. S. Huang and X. Han, "On improving the accuracy of structured light systems," Proc. SPIE **6382**, 63820H (2006).